

# Accessing Multi-triplons in Spin Ladders using Resonant Inelastic X-ray Scattering

Gary Ferkinghoff,<sup>1</sup> Leanna Müller,<sup>1</sup> Götz S. Uhrig,<sup>1</sup> Umesh Kumar,<sup>2</sup> and Benedikt Fauseweh<sup>2</sup>

<sup>1</sup>*Lehrstuhl für Theoretische Physik I, Technische Universität Dortmund,  
Otto-Hahn-Straße 4, 44221 Dortmund, Germany*

<sup>2</sup>*Theoretical Division, Los Alamos National Laboratory, Los Alamos, New Mexico 87545, USA*

(Dated: December 4, 2020)

Resonant inelastic x-ray scattering (RIXS) has proven a powerful tool to investigate dynamic magnetic correlations, yielding complementary insights compared to neutron scattering. A key issue is the interpretation of spectroscopic measurements in terms of quasi-particle excitations. In this paper we study the spin-conserving channel of RIXS spectra for two-leg quantum spin ladders using continuous unitary transformations. We find that multi-triplon continua and bound states are the leading contribution, opening new venues for observing and characterizing multi-triplons in quantum spin systems.

Exploring and identifying novel phases of matter is a central aim in modern solid-state physics. By identifying typical excitation spectra which can be related uniquely to the underlying phases by means of their elementary excitations, scattering experiments provide a unique tool for this purpose. Many exotic phases, such as disordered spin liquids, can be identified by their excitation spectrum, making theoretical corroboration important in the interpretation of such experiments.

A unique class of materials in this context are spin ladder compounds. During the last three decades, they have been the subject of great interest in the strongly correlated community. Ladder compounds are intermediate between one-dimensional and two-dimensional systems, offering a platform to understand many novel phenomena common to these systems, such as fractionalization, quantum criticality, and even superconductivity.

Traditionally, inelastic neutron scattering (INS) has allowed one to study the spin dynamics in strongly correlated materials. For instance, one-triplon dynamics was observed in the ladder compound,  $\text{Sr}_{14}\text{Cu}_{24}\text{O}_{41}$  cuprates [1] following earlier theoretical predictions [2, 3]. More recently, confined spinons were observed in weakly coupled spin ladder compounds,  $\text{CaCu}_2\text{O}_3$  [4] following the predictions in Ref. [5]. The field induced quantum critical point in  $(\text{C}_5\text{H}_{12}\text{N})_2\text{CuBr}_4$  was investigated in Ref. [6]. Another major breakthrough in a ladder compound has been the observation of superconductivity in  $\text{Sr}_{0.4}\text{Ca}_{13.6}\text{Cu}_{24}\text{O}_{41.84}$  [7], again preceded by a theoretical study [8].

Several studies in the past have tried to understand the multi-triplon dynamics in ladder compounds. Using INS,  $S = 1$  two-triplon states were observed in  $\text{La}_4\text{Sr}_{10}\text{Cu}_{24}\text{O}_{41}$  [9] and analyzed using the continuous unitary transformation (CUT) method.

In the recent years, resonant inelastic x-ray scattering (RIXS) has become an important complementary tool to study spin dynamics [10]. It has allowed observation of paramagnons in doped two-dimensional (2D) cuprates [11], spin-orbital separation [12] multi-spinon outside of two-spinon continua [13, 14] in a one-dimensional (1D) cuprate, inaccessible to INS probe. To

the best of our knowledge, only one RIXS experiment has been reported on a ladder cuprate,  $\text{Sr}_{14}\text{Cu}_{24}\text{O}_{41}$  [15]. The RIXS signal was interpreted as  $S = 0$  two-triplon states, before realizing that RIXS can indeed measure single spin-flip excitations [16, 17]. Subsequent numerical studies reported that these spectra should indeed be dominated by  $S = 1$  two-triplon states [18, 19]. It is also known that RIXS spectra can be resolved into spin-conserving ( $\Delta S = 0$ ) and spin non-conserving ( $\Delta S \neq 0$ ) at the Cu  $L_3$  edge [20, 21], allowing for new challenges and opportunities. The spin-conserving channel is unique to RIXS and can be well captured by the dynamical exchange structure factor. Apart from a channel at the Cu  $L$ -edge, Cu  $K$ -edge and oxygen  $K$ -edge in cuprates consist of only spin conserving channels [13, 22].

One key issue in these studies is the interpretation of RIXS spectra in terms of single quasi-particle excitations, multi-particle continua, and (anti)-bound states. The Kramers-Heisenberg (KH) formalism captures the RIXS mechanism, which is usually evaluated using exact diagonalization on finite systems [14, 15, 23–25]. More recently density matrix renormalization group has also been developed to evaluate RIXS spectra using KH formalism [26]. Also, the KH formalism can be cast into simpler dynamical correlation functions under the ultra-fast core-hole lifetime (UCL) [27, 28] approximation. These dynamical correlation functions were also studied using numerical techniques [18, 19, 29]. While these numerical approaches can provide high-resolution spectral functions [30, 31], they do not yield an intrinsic physical understanding of the underlying processes and structure of the spectra. In contrast, the study of dynamical correlation functions using exact methods in the thermodynamic limit allow for a detailed characterization in terms of quasi-particle excitations. For example, analysis of the RIXS spectra of the 1D antiferromagnetic chain using Bethe Ansatz showed that its spin-conserving channel entirely fractionalizes into two-spinon states [32].

In this paper we study the spin-conserving channel of spin ladders as probed by RIXS. We use the CUT technique to obtain an effective model of the spin ladder in terms of triplons. CUT was used in a variety of problems, such

as the renormalization of the electron-phonon coupling [33, 34], dissipative systems [35], impurity problems [36], the 2D Hubbard model [37] as well as 1D [38, 39] and 2D [40] spin systems. It gives us direct access to the renormalized multiparticle interactions and spectral weights in the thermodynamic limit. Using this approach, we reveal how the RIXS response is sensitive to multiparticle excitations and bound states, which can not be captured by conventional INS experiments.

We study a spin model in a two-leg ladder geometry. The Hamiltonian reads

$$H = J_{\text{rung}} \sum_{i=1}^N \mathbf{S}_{i,1} \cdot \mathbf{S}_{i,2} + J_{\text{leg}} \sum_{i,\tau=1,2} \mathbf{S}_{i,\tau} \cdot \mathbf{S}_{i+1,\tau} \quad (1)$$

Here,  $\mathbf{S}_{i,\tau}$  is a spin operator at site  $i$  along the leg and on rung  $\tau = 0, 1$ ;  $J_{\text{leg}}(J_{\text{rung}})$  are the superexchange along the leg (rung) direction of the ladder, respectively. This model describes the spin dynamics of a number of strongly correlated ladder compounds at half-filling. To compute the RIXS response at the Cu  $L$ -edge of cuprates, we use the dynamical correlation functions given by the UCL approximation [28]. At this edge, the spectra consist of the non-spin-conserving channel (NSC) and the spin-conserving channel (SC). The NSC is dominated by the dynamical spin structure factor (DSF) which is also accessible to INS. We provide data for the DSF in the Supplemental Material [41]. The SC channel can be well captured by the dynamical spin-exchange structure factor (DESF) given by

$$S^{\text{exch}}(\mathbf{q}, \omega) = \frac{1}{N} \sum_f |\langle f | \sum_{i,\tau} e^{i\mathbf{q}\mathbf{R}_{i,\tau}} O_{i,\tau}^{\text{exch}} | g \rangle|^2 \times \delta(E_f - E_g + \omega) \quad (2)$$

where  $O_{i,\tau}^{\text{exch}} = \mathbf{S}_{i,\tau} \cdot [J_{\text{leg}}(\mathbf{S}_{i+1,\tau} + \mathbf{S}_{i-1,\tau}) + J_{\text{rung}}\mathbf{S}_{i,\bar{\tau}}]$  is the spin exchange observable.  $|g\rangle$  and  $|f\rangle$  are the ground, and final states with energies  $E_g$  and  $E_f$  respectively, and  $\omega$  is the energy loss to the system. Fig. 1 illustrates the spin excitation via double spin-flip in the SC channel.

In order to evaluate the SC contribution to the RIXS spectra we decouple the interacting multi-triplon sectors from each other by applying a CUT to the Hamiltonian and the relevant observables which is systematically controlled up to high order in the expansion parameter  $x = J_{\text{leg}}/J_{\text{rung}}$ . This mapping renders the subsequent computations for few quasi-particles possible, as the effective Hamiltonian is decomposed into  $n$ -particle irreducible parts. The starting point for this approach is the strong-coupling regime, in which spin singlets are formed on the rungs. We then reformulate (1) in terms of triplon creation and annihilation operators  $t_i^\alpha |s\rangle = |t_i^\alpha\rangle$ , where  $|s\rangle$  is the singlet ground state for  $x = 0$  and  $|t_i^\alpha\rangle$  is an  $S = 1$  triplet state of flavor  $\alpha \in \{x, y, z\}$  on rung  $i$ . Explicit expressions for the Hamiltonian and the observables in the triplon language are given in the Supplemental Material [41]. We compute  $H_{\text{eff}}$  and the corresponding effective observables up to order 10 in the directly evaluated

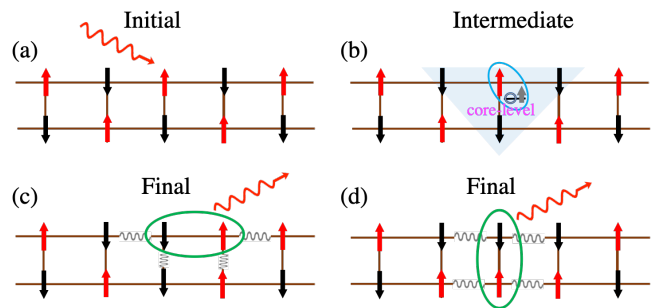


FIG. 1: Schematics for double spin-flips in the spin ladder. The photon interacts with a local site (a), the local core-hole potential in the spin-conserving channel perturbs the system locally (b) and allows for excitations via double spin-flips along the chain (c) and the rung (d).

enhanced perturbative CUT (deepCUT). The deepCUT approach allows for a non-perturbative evaluation of  $H_{\text{eff}}$  and was proven to yield reliable results for the spin ladder up to  $x = 3$  [42], while being stable even in the presence of frustration [43, 44]. We choose a particle conserving generator  $m:n$ , which decouples only the first  $m$  quasi-particle sectors from all other sectors  $n$  [45, 46]. In this paper we decouple the zero-, one-, two- and three-triplon sector [41]. Based on the effective observables obtained from the CUT we use a Lanczos algorithm to compute a continued fraction expansion of the DSF and the DESF [41]. This allows for negligible finite size effects and at the same time identifies the important physical processes that contribute to the spectral functions. The accuracy of the CUT approach is examined by comparing it to lower order CUT calculations as well as to results from exact diagonalization on finite systems in the Supplemental Material [41].

We compute the RIXS response for the values  $x = \{0.25, 0.5, 1.2, 2.0\}$ . This choice covers the strong-, intermediate- and weak-coupling regime. The value  $x = 1.2$  is included because it is relevant for the ladder cuprate  $\text{Sr}_{14}\text{Cu}_{24}\text{O}_{41}$ . In the strong-coupling regime, the system is dimerized on the rungs. The elementary excitations are rung triplons which couple due to the leg coupling, letting the triplons hop and interact. In the weak-coupling regime  $x \gg 1$  the physical picture is that of two weakly coupled spin chains, with fractional spinon excitations. For any finite rung coupling the spin gap is finite, because the spinons are subject to a confining potential. Strong- and weak-coupling regimes are separated by a crossover, not a quantum phase transition. This allows the CUT approach to accurately describe the spin dynamics even for  $J_{\text{leg}} > J_{\text{rung}}$  in terms of multi-triplon contributions. In this paper we focus on the SC channel of RIXS, which is inaccessible to INS. In Figure 2 and 3 we show the results for the SC channel as function of momentum  $\mathbf{q} = (q_x, q_y)$  and energy  $\omega$ . Note that  $q_x = [0, \pi)$  denotes the continuous direction along the ladder, while  $q_y$  is oriented along the rungs.  $q_y$  takes the discrete values  $\{0, \pi\}$ .

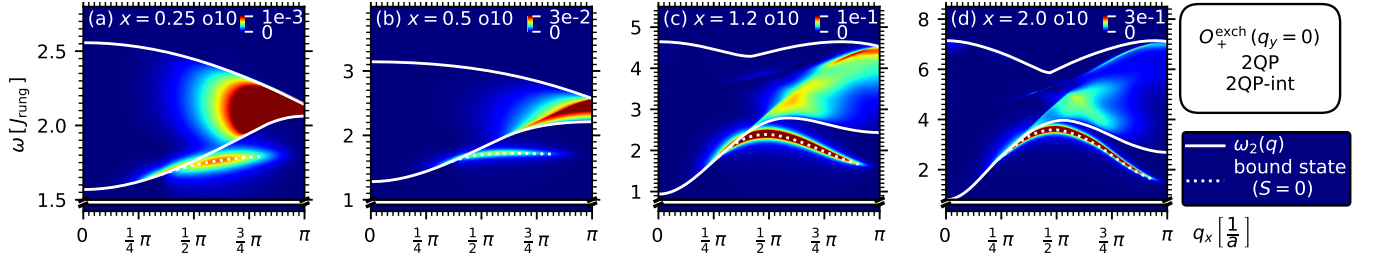


FIG. 2: RIXS response in the SC channel for  $q_y = 0$ . Results from the deepCUT in order 10 for the parameter  $x$  using the  $2:n$  generator. The solid white line shows the boundary of the two-triplon continuum and the dashed white line shows the  $S = 0$  bound state, broadened with a Lorentzian of width  $0.05J_{\text{rung}}$ .

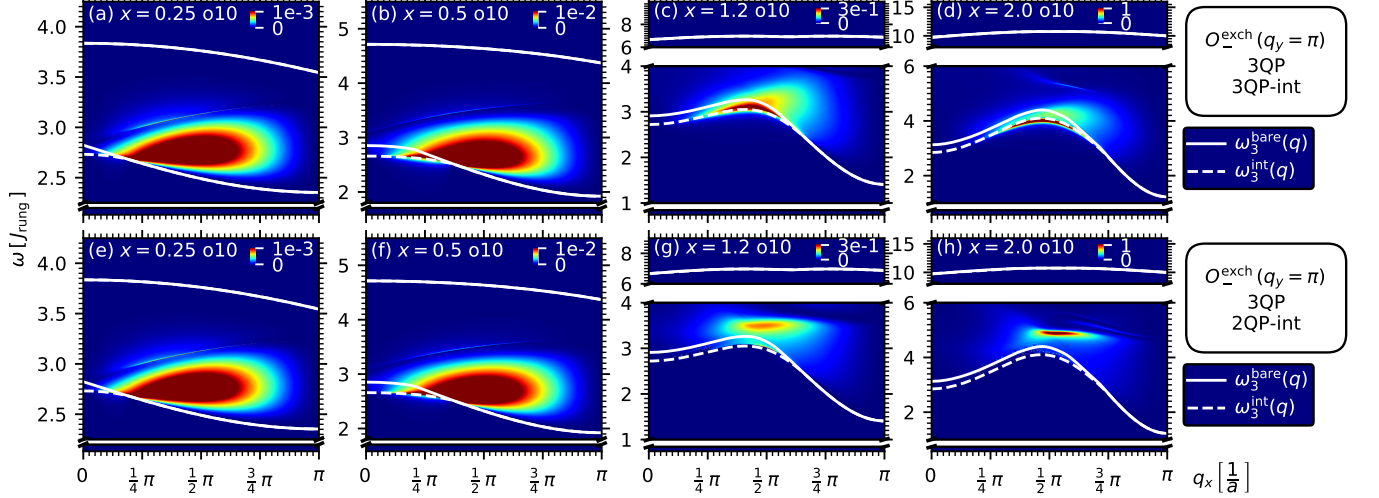


FIG. 3: RIXS response in the SC channel for  $q_y = \pi$ . (a)-(d) results from the mixed deepCUT calculations,  $2:n$  generator in order 10 for the single- and two-triplon matrix elements,  $3:n$  generator in order  $\geq 5$  for the three-triplon matrix elements ( see Supplemental Material [41]). The effective observable was computed with the  $3:n$  generator. (e)-(h) results from the  $2:n$  deepCUT calculations in order 10 excluding irreducible three-triplon interactions.

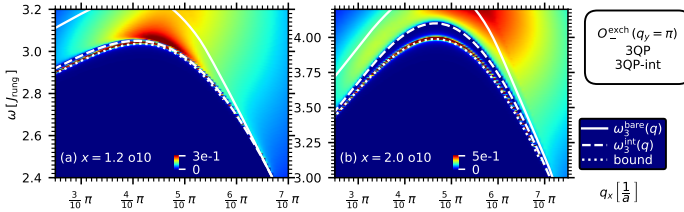


FIG. 4: RIXS response in the SC channel for  $q_y = \pi$ . Detailed view of the lower three-triplon boundary and the formation of a three-triplon bound state outside of the continuum, broadened with a Lorentzian of width  $0.0005J_{\text{rung}}$ .

The system has a reflection symmetry  $\mathcal{P}$  around the center line of the ladder along the  $x$  direction. The corresponding parity is a conserved quantity before and after the CUT. This implies that the channels with even and odd numbers of triplons are decoupled and that observables that have a even (odd) parity for  $x = 0$  will inject an even (odd) number of triplons for any  $x$  [47]. Similar to the DSF, the  $q_y = 0$  results in Fig. 2 for the DESF is dominated by the two-triplon contributions, due

to the even parity of the observable. For fixed total momentum the two triplons form a spectral continuum as function of energy. The boundary of the continuum are determined by the single-triplon dispersion and are indicated in the plots as solid white lines. Additionally two-triplon bound states are formed, due to triplon-triplon interaction. The dispersion of these bound states depends on the total spin of the two triplons. Due to the selection rule  $\Delta S = 0$  the  $S = 1$  bound state is forbidden in the spectra. Instead the  $S = 0$  bound state emerges below the two-triplon continuum. Importantly this bound states is *lower* in energy than the  $S = 1$  bound state [41, 47, 48]. This bound state was first reported in the ladder material  $(\text{Ca},\text{La})_{14}\text{Cu}_{24}\text{O}_{41}$  using optical two-triplon-plus-phonon absorption spectroscopy [49]. In the strong-coupling regime  $x < 1.2$ , the dominating spectral weight is in the continuum at  $q_x \approx \pi$ , with a smaller fraction of the spectral weight in the bound state. The continuum itself is rather featureless. This changes upon approaching the weak-coupling limit. Here the bound state holds the leading contribution in the two-triplon channel around  $q_x = \pi/2$  and the continuum shows more

pronounced features. Specifically there is a strong aggregation of spectral weight at a mid-band singularity. This singularity can be traced back to the lower boundary of the two-spinon continuum in the weak-coupling limit [47] and is a precursor of fractionalized excitations. This feature is also present in the DSF, but much less pronounced. In the Supplemental Material we also compare the two- and four-triplon sector [41].

In Fig. 3 we investigate the RIXS response for  $q_y = \pi$ . Here the effective observable has odd parity, but does not couple to the single-triplon channel, because the single triplon is a  $\Delta S = 1$  excitation. The leading contributions comes instead from the three-triplon sector.

For the results shown in Fig. 3(a)-(d) we use a mixed Hamiltonian calculation, i.e., the irreducible single- and two-triplon terms in the Hamiltonian are computed up to order 10, while the three-triplon interactions are computed up to at least order 5, see also Supplemental Material [41, 47]. Higher order calculations in the three-triplon sector are not accessible within the deepCUT approach due to a divergence in the flow equations resulting from the strong quasi-particle overlap.

The CUT approach allows us to disentangle the effect of different quasi-particle spaces. Thus, we computed a second data set, where we performed a  $2:n$  calculation and neglect the three-triplon interactions for the computation of the RIXS response. Comparing the results from Fig. 3 (a)-(d) with the  $2:n$  calculations in Fig. 3 (e)-(h) we can clearly distinguish the spectral features induced by three-triplon interactions from pure two-triplon effects.

In the strong-coupling regime, e.g., for  $x = 0.25$  and  $x = 0.5$ , the response is mostly centered around  $q_x = \pi/2$  in the middle of the three-triplon continuum. Increasing the leg coupling shifts spectral weight towards the lower boundary of the continuum. There is no significant difference between the  $3:n$  and the  $2:n$  calculations indicating that the irreducible three-triplon interactions are negligible for small values of  $x$ . However this changes drastically in the weak-coupling regime.

For  $x > 0.5$  the calculations including three-triplon interactions, Fig. 3 c) and d), predict that most of the weight is in a region of the three-particle continuum which is outside the bare three-triplon continuum. The bare boundaries of the three-triplon continuum are computed based on the energy of three separated triplons and total momentum conservation. However, due to the bound states in the two-triplon sector, the boundaries of the three-triplon continuum are modified, see the dashed white line. Our results show that the spectral distribution is strongly affected by the three-triplon interactions, leading to a sharp response at the lower boundary. In contrast the  $2:n$  calculations predict that the dominating spectral weight is within the bare three-triplon continuum. This suggests that a three-triplon bound state with a very small energy separation from the three-triplon continuum can exist similar to multi-magnon bound states discovered only very recently [50]. Indeed a closer inspection reveals, that a single eigenvalue of the effective

Hamiltonian lies outside of the three triplon continuum for  $x = 1.2$  and  $x = 2.0$  and forms a three-triplon bound state, see Fig. 4. Our analysis reveals, that the bound state exists for  $q_x \geq 0$  until it merges with the continuum at  $q_x \approx 0.65\pi$ . Depending on  $q_x$ , the bound states carries a significant portion of the total weight, i.e., up to 33 % for  $x = 1.2$  and  $q_x \approx 0.39\pi$ . Since the energy difference to the boundary is very small, i.e.,  $\approx 0.05J_{\text{runng}}$ , this bound state cannot be distinguished from the three-triplon continuum in exact diagonalization, see Supplemental Material [41]. Previously multi-triplon bound states have been reported in strongly frustrated spin ladders [51], but so far not in the unfrustrated case for more than two triplons. Thus our calculations prove a significant three-triplon interaction effect onto the spectra, that gets even stronger as we enter into the weak-coupling regime. Here RIXS provides a unique opportunity to study these multi-triplon interaction effects in real materials.

In this paper we investigated the RIXS response of spin ladder systems. With the capability of RIXS to distinguish spin conserving and spin non-conserving channels new insights into these systems are possible. Our results show, that the spin-conserving channel provides a promising approach to measure multi-triplon excitations, including  $S = 0$  bound states, which are inaccessible to INS experiments. We could further identify precursors of fractionalized physics in the weak-coupling regime within the spectra, which are much more pronounced in the SC channel. For  $q_y = \pi$  we showed, that the three-triplon sector is the leading contribution to the SC channel. Here we clearly identified signatures of strong irreducible three-triplon interactions in the weak-coupling regime, with the formation of a so far unreported three-triplon bound state for  $x = 1.2$  and  $x = 2.0$ .

From the theoretical perspective we showed, that the CUT approach is capable of delivering high resolution predictions for RIXS spectra paired with the ability to classify contributions according to particle number and to identify three-triplon effects from three-triplon interactions. Thus the predictive power of systematically controlled disentanglement of quasi-particle sectors provides the physical understanding in terms of effective models. Many possible future studies are implied by our results. The effective models from CUT provide a unique opportunity to describe and predict future RIXS experiments on quantum magnets and spin liquids. The approach is also compatible with finite temperature [52–55] and applied magnetic fields, in which multiparticle excitations have been reported [56].

It will be interesting to apply the CUT approach to compute the RIXS response in the two dimensional Heisenberg model. Recent studies suggest that the attractive magnon-magnon interaction in this system gives rise to the formation of a ‘‘Higgs’’ resonance [57–59]. This resonance has an indirect effect on the single magnon propagation in the DSF. It would be intriguing to investigate, if the RIXS response is directly sensitive to the Higgs mode and provides complementary information.

This work was supported by the U.S. DOE NNSA under Contract No. 89233218CNA000001 via the LANL LDRD

Program. G.S.U. is supported by the DFG under project No. UH90/14-1.

- 
- [1] R. S. Eccleston, M. Uehara, J. Akimitsu, H. Eisaki, N. Motoyama, and S.-i. Uchida, *Phys. Rev. Lett.* **81**, 1702 (1998).
- [2] T. Barnes, E. Dagotto, J. Riera, and E. S. Swanson, *Phys. Rev. B* **47**, 3196 (1993).
- [3] S. Gopalan, T. M. Rice, and M. Sigrist, *Phys. Rev. B* **49**, 8901 (1994).
- [4] B. Lake, A. M. Tsvelik, S. Notbohm, D. Alan Tennant, T. G. Perring, M. Reehuis, C. Sekar, G. Krabbes, and B. Büchner, *Nat. Phys.* **6**, 50 (2010).
- [5] D. G. Shelton, A. A. Nersesyan, and A. M. Tsvelik, *Phys. Rev. B* **53**, 8521 (1996).
- [6] D. Blosser, V. K. Bhartiya, D. J. Voneshen, and A. Zheludev, *Phys. Rev. Lett.* **121**, 247201 (2018).
- [7] M. Uehara, T. Nagata, J. Akimitsu, H. Takahashi, N. Môri, and K. Kinoshita, *J. Phys. Soc. Japan* **65**, 2764 (1996).
- [8] E. Dagotto, J. Riera, and D. Scalapino, *Phys. Rev. B* **45**, 5744 (1992).
- [9] S. Notbohm, P. Ribeiro, B. Lake, D. A. Tennant, K. P. Schmidt, G. S. Uhrig, C. Hess, R. Klingeler, G. Behr, B. Büchner, M. Reehuis, R. I. Bewley, C. D. Frost, P. Manuel, and R. S. Eccleston, *Phys. Rev. Lett.* **98**, 027403 (2007).
- [10] L. J. P. Ament, M. van Veenendaal, T. P. Devereaux, J. P. Hill, and J. van den Brink, *Rev. Mod. Phys.* **83**, 705 (2011).
- [11] M. Le Tacon, G. Ghiringhelli, J. Chaloupka, M. M. Sala, V. Hinkov, M. W. Haverkort, M. Minola, M. Bakr, K. J. Zhou, S. Blanco-Canosa, C. Monney, Y. T. Song, G. L. Sun, C. T. Lin, G. M. De Luca, M. Salluzzo, G. Khalullin, T. Schmitt, L. Braicovich, and B. Keimer, *Nat. Phys.* **7**, 725 (2011).
- [12] J. Schlappa, K. Wohlfeld, K. J. Zhou, M. Mourigal, M. W. Haverkort, V. N. Strocov, L. Hozoi, C. Monney, S. Nishimoto, S. Singh, A. Revcolevschi, J.-S. Caux, L. Patthey, H. M. Rønnow, J. van den Brink, and T. Schmitt, *Nature* **485**, 82 (2012).
- [13] J. Schlappa, U. Kumar, K. J. Zhou, S. Singh, M. Mourigal, V. N. Strocov, A. Revcolevschi, L. Patthey, H. M. Rønnow, S. Johnston, and T. Schmitt, *Nat. Commun.* **9**, 5394 (2018).
- [14] U. Kumar, A. Nocera, E. Dagotto, and S. Johnston, *New J. Phys.* **20**, 073019 (2018).
- [15] J. Schlappa, T. Schmitt, F. Vernay, V. N. Strocov, V. Ilakovac, B. Thielemann, H. M. Rønnow, S. Vanishri, A. Piazzalunga, X. Wang, L. Braicovich, G. Ghiringhelli, C. Marin, J. Mesot, B. Delley, and L. Patthey, *Phys. Rev. Lett.* **103**, 047401 (2009).
- [16] L. J. P. Ament, G. Ghiringhelli, M. M. Sala, L. Braicovich, and J. van den Brink, *Phys. Rev. Lett.* **103**, 117003 (2009).
- [17] L. Braicovich, J. van den Brink, V. Bisogni, M. M. Sala, L. J. P. Ament, N. B. Brookes, G. M. De Luca, M. Salluzzo, T. Schmitt, V. N. Strocov, and G. Ghiringhelli, *Phys. Rev. Lett.* **104**, 077002 (2010).
- [18] U. Kumar, A. Nocera, E. Dagotto, and S. Johnston, *Phys. Rev. B* **99**, 205130 (2019).
- [19] T. Nagao and J.-i. Igarashi, *Phys. Rev. B* **85**, 224436 (2012).
- [20] V. Bisogni, S. Kourtis, C. Monney, K. Zhou, R. Kraus, C. Sekar, V. Strocov, B. Büchner, J. van den Brink, L. Braicovich, T. Schmitt, M. Daghofer, and J. Geck, *Phys. Rev. Lett.* **112**, 147401 (2014).
- [21] R. Fumagalli, L. Braicovich, M. Minola, Y. Y. Peng, K. Kummer, D. Betto, M. Rossi, E. Lefrançois, C. Morawe, M. Salluzzo, H. Suzuki, F. Yakhov, M. Le Tacon, B. Keimer, N. B. Brookes, M. M. Sala, and G. Ghiringhelli, *Phys. Rev. B* **99**, 134517 (2019).
- [22] D. S. Ellis, J. Kim, J. P. Hill, S. Wakimoto, R. J. Birge-neau, Y. Shvyd'ko, D. Casa, T. Gog, K. Ishii, K. Ikeuchi, A. Paramekanti, and Y.-J. Kim, *Phys. Rev. B* **81**, 085124 (2010).
- [23] S. Kourtis, J. van den Brink, and M. Daghofer, *Phys. Rev. B* **85**, 064423 (2012).
- [24] K. Wohlfeld, S. Nishimoto, M. W. Haverkort, and J. van den Brink, *Phys. Rev. B* **88**, 195138 (2013).
- [25] U. Kumar, A. Nocera, G. Price, K. Stiwinter, S. Johnston, and T. Datta, *Phys. Rev. B* **102**, 075134 (2020).
- [26] A. Nocera, U. Kumar, N. Kaushal, G. Alvarez, E. Dagotto, and S. Johnston, *Sci. Rep.* **8**, 11080 (2018).
- [27] L. J. P. Ament, F. Forte, and J. van den Brink, *Phys. Rev. B* **75**, 115118 (2007).
- [28] C. Jia, K. Wohlfeld, Y. Wang, B. Moritz, and T. P. Devereaux, *Phys. Rev. X* **6**, 021020 (2016).
- [29] F. Forte, M. Cuoco, C. Noce, and J. van den Brink, *Phys. Rev. B* **83**, 245133 (2011).
- [30] D. Schmidiger, P. Bouillot, S. Mühlbauer, S. Gvasaliya, C. Kollath, T. Giamarchi, and A. Zheludev, *Phys. Rev. Lett.* **108**, 167201 (2012).
- [31] M. Nayak, D. Blosser, A. Zheludev, and F. Mila, *Phys. Rev. Lett.* **124**, 087203 (2020).
- [32] A. Klausner, J. Mossel, J.-S. Caux, and J. van den Brink, *Phys. Rev. Lett.* **106**, 157205 (2011).
- [33] A. Mielke, *EPL* **40**, 195 (1997).
- [34] A. Mielke, *Ann. d. Phys.* **509**, 215 (1997).
- [35] T. Stauber and A. Mielke, *Phys. Lett. A* **305**, 275 (2002).
- [36] J. Krones and G. S. Uhrig, *Phys. Rev. B* **91**, 125102 (2015).
- [37] Hankevych, V. and Wegner, F., *Eur. Phys. J. B* **31**, 333 (2003).
- [38] C. Knetter and G. S. Uhrig, *Eur. Phys. J. B* **13**, 209 (2000).
- [39] B. Fauseweh and G. S. Uhrig, *Phys. Rev. B* **87**, 184406 (2013).
- [40] C. Knetter and G. S. Uhrig, *Phys. Rev. Lett.* **92**, 027204 (2004).
- [41] See Supplemental Material at [URL will be inserted by publisher] for details on Triplon representation; Continuous Unitary Transformation; Lanczos tridiagonalization; Non spin conserving RIXS response and Numerical details.
- [42] H. Krull, N. A. Drescher, and G. S. Uhrig, *Phys. Rev. B* **86**, 125113 (2012).

- [43] L. Splinter, N. A. Drescher, H. Krull, and G. S. Uhrig, *Phys. Rev. B* **94**, 155115 (2016).
- [44] M. Malki, L. Müller, and G. S. Uhrig, *Phys. Rev. Research* **1**, 033197 (2019).
- [45] Knetter, C. and Uhrig, G. S., *Eur. Phys. J. B* **13**, 209 (2000).
- [46] T. Fischer, S. Duffe, and G. S. Uhrig, *New J. Phys.* **12**, 033048 (2010).
- [47] C. Knetter, K. P. Schmidt, M. Grüninger, and G. S. Uhrig, *Phys. Rev. Lett.* **87**, 167204 (2001).
- [48] S. Trebst, H. Monien, C. J. Hamer, Z. Weihong, and R. R. P. Singh, *Phys. Rev. Lett.* **85**, 4373 (2000).
- [49] M. Windt, M. Grüninger, T. Nunner, C. Knetter, K. P. Schmidt, G. S. Uhrig, T. Kopp, A. Freimuth, U. Ammerahl, B. Büchner, and A. Revcolevschi, *Phys. Rev. Lett.* **87**, 127002 (2001).
- [50] Z. Wang, J. Wu, W. Yang, A. K. Bera, D. Kamenskyi, A. T. M. N. Islam, S. Xu, J. M. Law, B. Lake, C. Wu, and A. Loidl, *Nature* **554**, 219 (2018).
- [51] A. Honecker, F. Mila, and B. Normand, *Phys. Rev. B* **94**, 094402 (2016).
- [52] B. Fauseweh, J. Stolze, and G. S. Uhrig, *Phys. Rev. B* **90**, 024428 (2014).
- [53] E. S. Klyushina, A. C. Tiegel, B. Fauseweh, A. T. M. N. Islam, J. T. Park, B. Klemke, A. Honecker, G. S. Uhrig, S. R. Manmana, and B. Lake, *Phys. Rev. B* **93**, 241109 (2016).
- [54] B. Fauseweh, F. Groitl, T. Keller, K. Rolfs, D. A. Tennant, K. Habicht, and G. S. Uhrig, *Phys. Rev. B* **94**, 180404 (2016).
- [55] B. Fauseweh and G. S. Uhrig, *Phys. Rev. B* **96**, 115150 (2017).
- [56] S. Ward, M. Mena, P. Bouillot, C. Kollath, T. Giamarchi, K. P. Schmidt, B. Normand, K. W. Krämer, D. Biner, R. Bewley, T. Guidi, M. Boehm, D. F. McMorrow, and C. Rüegg, *Phys. Rev. Lett.* **118**, 177202 (2017).
- [57] T. Ying, K. P. Schmidt, and S. Wessel, *Phys. Rev. Lett.* **122**, 127201 (2019).
- [58] M. Powalski, G. S. Uhrig, and K. P. Schmidt, *Phys. Rev. Lett.* **115**, 207202 (2015).
- [59] M. Powalski, K. P. Schmidt, and G. S. Uhrig, *SciPost Phys.* **4**, 001 (2018).